Probing the Stop Sector and the Sanity of the MSSM with the Higgs Boson at the LHC

Radovan Dermíšek[a] and Ian Low[b]

[a] *School of Natural Sciences, Institute for Advanced Study, Princeton, NJ 08540*

[b] *Department of Physics and Astronomy, University of California, Irvine, CA 92697*

Abstract

We propose using the lightest CP-even Higgs boson in the minimal supersymmetric standard model (MSSM) to probe the stop sector. Unlike measuring stop masses in production/decay processes which requires knowledge of masses and mixing angles of other superparticles, the strategy depends little on supersymmetric parameters other than those in the stop sector in a large region of parameter space. We show that measurements of the Higgs mass and the production rate in the gluon fusion channel, the dominant channel at the LHC, allow for determination of two parameters in the stop mass-squared matrix, including the off-diagonal mixing term. This proposal is very effective when stops are light and their mixing is large, which coincides with the region where the electroweak symmetry breaking is minimally fine tuned. We also argue that a lightest CP-even Higgs mass in the upper range of allowed values and a production rate significantly smaller than in the standard model would be difficult to reconcile within the MSSM, except in extreme (insane) corners of the parameter space.

I. INTRODUCTION

Supersymmetry (SUSY) is usually considered the leading candidate for physics beyond the standard model. Among many virtues of SUSY, perhaps the most prominent ones are the stabilization of the electroweak scale up to very high energies such as the grand unification scale and the possibility of radiatively driven electroweak symmetry breaking (EWSB). However, neither the Higgs boson nor any superpartners have been found in collider experiments so far, and it is discomforting to realize that majority of natural parameter space of MSSM has been ruled out by current experimental limits on the Higgs mass [1], leaving us with the parameter space where EWSB is achieved with fine tuning of soft SUSY breaking parameters at a few percent level. [1]

The EWSB and the mass of the Higgs boson in the MSSM are tightly connected with the stop sector: stop mass squared parameters, $m^2_{\tilde{t}_L}$ and $m^2_{\tilde{t}_R}$, and the mixing, $X_t = A_t - \mu/\tan\beta$, where A_t is the top soft trilinear coupling, μ is the supersymmetric Higgs mass and $\tan\beta = v_u/v_d$ is the ratio of the vacuum expectation values of up-type and down-type Higgs bosons. These parameters enter the calculation of physical stop masses, $m_{\tilde{t}_1}$ and $m_{\tilde{t}_2}$, which is what we measure in experiments. Information about the mixing is not given from mass eigenstates. The splitting between $m_{\tilde{t}_1}$ and $m_{\tilde{t}_2}$ can originate either from the difference between $m^2_{\tilde{t}_L}$ and $m^2_{\tilde{t}_R}$ or from large mixing. However, the mixing in the stop sector is crucial for the Higgs boson mass. In MSSM the mass of the lightest CP-even Higgs mass is bounded at the tree-level by the Z boson mass, $m_h \leq m_Z|\cos 2\beta|$. In order to lift the Higgs mass above the LEP limit $m_h \geq 114$ GeV, radiative corrections from stops are required to be large, which then implies either stop masses heavier than about 900 GeV for moderate mixing, or large stop mixing for fairly light stop masses. Indeed the region of large mixing, $X_t/m_{\tilde{t}_{L,R}} \simeq \pm 2$, and stop masses $m_{\tilde{t}_L} \simeq m_{\tilde{t}_R} \simeq 300$ GeV minimizes the fine tuning of EWSB while satisfying the limit on the Higgs mass. There has been some effort to realize the large mixing scenario in models, see e.g. Refs. [3, 4, 5, 6], in order to address the naturalness issue of MSSM. It goes without saying that determining parameters of the stop sector precisely in collider experiments will be of great importance for understanding the EWSB, the Higgs mass and the internal consistency of MSSM. [2]

[1] For recent discussion of fine tuning in EWSB see e.g. Refs. [2, 3, 4, 5, 6].

[2] It is important to note that the discussion in this paragraph is specific to the MSSM. In models with more

So how does one measure stop masses and the mixing angle? This is a simple question without a simple answer. In the MSSM with R-parity the lightest supersymmetric particle (LSP) is stable. In a large class of models the lightest neutralino is (or can be) the LSP and a good candidate for dark matter. In collider experiments the lightest neutralino (being stable and electrically neutral) will escape direct detection and result in events with missing transverse energy (E_T). Due to R-parity superparticles need to be pair-produced and they eventually cascade-decay into the LSP plus standard model particles. Thus a typical event for the production and decay of superparticles is multi-jet and multi-lepton with large missing E_T. In the end the stop, if produced, is never directly observed in collider detectors. Any reconstruction of masses and mixing angle in the production/decay processes has to rely on the visible decay product and missing E_T.

At the Large Hadron Collider (LHC) various reasons complicate the measurement of masses and mixing angle in the production/decay process. First, the large missing E_T makes event-by-event reconstruction of masses impossible; one has to resort to measuring kinematic endpoints and edges of invariant mass distributions of final particles. The position of such endpoints and edges is sensitive to masses of all particles involved in the decay chain, including the LSP which escapes detection. Second, at hadron colliders it is the partons inside the proton that collide with each other and the center-of-mass energy is not a known quantity. Thus there is no kinematic constraint to impose in the longitudinal direction of the collider. Third, because of long decay chains of SUSY particles there are usually many jets and leptons in the final state, leading to large combinatoric factors. Previous studies [7] showed that in the end it is quite a complicated and elaborate analysis to extract mass parameters in the production/decay processes, and the outcome crucially depends on knowing the mass and nature of other particles in the decay chain such as charginos and neutralinos. For stops, there is an added layer of complexity because decay of stops sometimes involve top quarks, which require extra efforts to identify.

In this paper we propose an approach, complimentary to studying the production/decay processes of stops, that does not require prior knowledge of the mass and mixing angle of other superparticles. The proposal is to use properties of the lightest CP-even Higgs boson

complicated Higgs sector, the mass of the Higgs boson can receive additional contributions or the 114 GeV limit on the Higgs mass might not apply due to modified Higgs decays. See e.g. Ref. [2] for related discussion.

in the MSSM to extract parameters in the stop sector. At the LHC the Higgs boson is produced dominantly through the gluon fusion process $gg \to h$ and subsequently decays into other standard model particles. By measuring the invariant mass of the decay products it is possible to determine the Higgs mass precisely. As it turns out in the MSSM both the gluon fusion production rate and the Higgs mass are sensitive only to parameters in the stop sector and not to masses and mixing of other superpartners. The only exception to this is the large $\tan\beta$ region where contributions from sbottom sector to both the Higgs mass and the gluon fusion rate can be significant. Furthermore, we will demonstrate that, if the variables are chosen appropriately, the Higgs mass and the gluon fusion rate depend on only two out of the three parameters in the mass matrix; the dependence on the third parameter is negligible in a significant region of parameter space. Therefore with two measurements in the Higgs sector we are able to extract two parameters in the stop mass-squared matrix, including the mixing term X_t.

There is also an interesting possibility that the two measurements (the Higgs mass and the gluon production rate) would point to mutually inconsistent values of stop masses and mixing, even after taking into account the current (large) estimates of experimental and theoretical errors. This is the case for a large Higgs mass $m_h \gtrsim 130$ GeV and a significantly reduced production rate in the gluon fusion channel. Even though, taken separately, these two measurements are perfectly allowed in the MSSM, we will argue that the combined scenario is very difficult to reconcile except in some extreme and insane corners of the parameter space. Finally, in every SUSY breaking scenario in which $m^2_{\tilde{t}_L}$ and $m^2_{\tilde{t}_R}$ are related to each other in any specific way, and in addition parameters in the sbottom sector are related to parameters in the stop sector, our procedure can be used to fix the parameters of the model, or it could possibly rule out the scenario if the measured value of the Higgs mass and the gluon production rate are impossible to satisfy for any choice of parameters.

II. THE STOP SECTOR IN MSSM

The stop mass-squared matrix in MSSM in the flavor basis $(\tilde{t}_L, \tilde{t}_R)$ is given by [8]

$$M^2_{\tilde{t}} = \begin{pmatrix} m^2_{\tilde{t}_L} + m^2_t + D^t_L & m_t X_t \\ m_t X_t & m^2_{\tilde{t}_R} + m^2_t + D^t_R \end{pmatrix}, \tag{1}$$

where

$$D_L^t = \left(\frac{1}{2} - \frac{2}{3}s_w^2\right) m_Z^2 \cos 2\beta, \tag{2}$$

$$D_R^t = \frac{2}{3}s_w^2 m_Z^2 \cos 2\beta, \tag{3}$$

$$X_t = A_t - \frac{\mu}{\tan\beta}. \tag{4}$$

In the above s_w is the sine of Weinberg angle. From Eq. (1) we see that there are four free parameters in the stop mass matrix: $\tan\beta$ (through the dependence on $\cos 2\beta$), $m^2_{\tilde{t}_L}$, $m^2_{\tilde{t}_R}$, and X_t. Nevertheless, the dependence on $\tan\beta$ is rather weak because $m_Z^2 \ll m_t^2$. Furthermore, the mass of the lightest CP-even Higgs boson in MSSM is insensitive to $\tan\beta$ once $\tan\beta \gtrsim 10$, in which case $\cos 2\beta \sim 1$. In this way neither the Higgs mass nor the stop mass-squared matrix is dependent of $\tan\beta$. On the other hand, the off-diagonal mixing in the sbottom mass matrix,

$$m_b X_b = m_b(A_b - \mu \tan\beta), \tag{5}$$

becomes substantial when $\tan\beta \sim m_t/m_b$ and the supersymmetric Higgs mass μ is large simultaneously. In this situation the sbottom contribution to both the Higgs mass and the production rate in the gluon fusion channel could be significant [9, 10]. Therefore the region of parameter space we would like to focus on in this paper is:

- $10 \lesssim \tan\beta \lesssim m_t/m_b$,
- $|m_b\, \mu \tan\beta| \lesssim m^2_{\tilde{b}_L},\ m^2_{\tilde{b}_R}$,

for which our strategy will not depend on SUSY parameters other than those in the stop sector. In this case the stop mass matrix is controlled by three parameters $m^2_{\tilde{t}_L}$, $m^2_{\tilde{t}_R}$, and X_t. In addition we will be interested in the so-called "decoupling limit"[11], in which the lightest CP-even Higgs h is standard model-like in that its couplings to quarks and leptons approach the standard model value, and all other Higgs bosons in MSSM are much heavier than h and roughly degenerate. This is also the region where $\tan\beta$ is large and m_h maximized.

III. STOPS AND THE GLUON FUSION PRODUCTION

At hadron colliders the dominant production mechanism for the Higgs boson is the gluon fusion production [12]. The contributing Feynman diagram is shown in Fig. 1, in which it

is the top quark running in the loop. The gluon fusion production, being a loop induced process, is very sensitive to new physics, especially any new colored particles coupling to the Higgs significantly. In the MSSM there is only one such particle, the stop, whereas all the other colored superparticles have much smaller coupling to the lightest CP-even neutral Higgs due to small Yukawa couplings. Therefore in the MSSM the gluon fusion production rate of the lightest CP-even Higgs boson probes the stop sector and is insensitive to other parts of the spectrum.[3]

Obviously the gluon fusion production rate is directly proportional to the decay rate of $h \to gg$, for which the stop contribution at one-loop level has been computed [8]. The analytic expressions, including the top quark contribution, are

$$\Gamma(h \to gg) = \frac{G_F \alpha_s^2 m_h^3}{36\sqrt{2}\pi^3} \left| \frac{3}{4} A_{\frac{1}{2}}^h(\tau_t) + \sum_{i=1,2} \frac{3}{4} \frac{g_{h\tilde{t}_i\tilde{t}_i}}{m_{\tilde{t}_i}^2} A_0^h(\tau_{\tilde{t}_i}) \right|^2 , \tag{6}$$

where $\tau_i = m_h^2/(4m_i^2)$ and the form factors are

$$A_{\frac{1}{2}}^h(\tau) = \frac{2}{\tau^2}[\tau + (\tau - 1) f(\tau)] , \tag{7}$$

$$A_0^h(\tau) = -\frac{1}{\tau^2}[\tau - f(\tau)] , \tag{8}$$

$$f(\tau) = \begin{cases} \arcsin^2 \sqrt{\tau} & \tau \leq 1 \\ -\frac{1}{4}\left[\log \frac{1+\sqrt{1-\tau^{-1}}}{1-\sqrt{1-\tau^{-1}}} - i\pi\right]^2 & \tau > 1 \end{cases} . \tag{9}$$

Furthermore, $g_{h\tilde{t}_i\tilde{t}_i}$ is the coupling of the lightest CP-even Higgs boson to stop mass eigen-

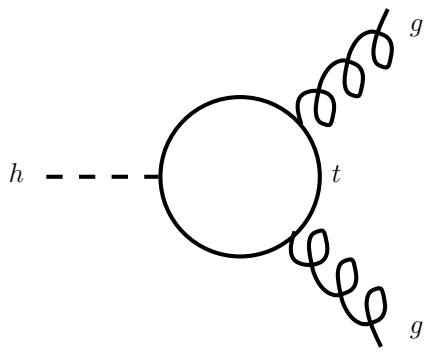

FIG. 1: Gluon fusion production of the Higgs boson in the standard model.

[3] The exception is, as commented earlier, for very large $\tan\beta \sim m_t/m_b$ when the sbottoms could be light and important [10].

states, normalized to $2(\sqrt{2}G_F)^{1/2}$,

$$g_{h\tilde{t}_1\tilde{t}_1} = m_Z^2 \cos 2\beta \left(\frac{1}{2}\cos^2\theta_t - \frac{2}{3}s_w^2 \cos 2\theta_t\right) + m_t^2 - \frac{1}{2}m_t X_t \sin 2\theta_t, \tag{10}$$

$$g_{h\tilde{t}_2\tilde{t}_2} = m_Z^2 \cos 2\beta \left(\frac{1}{2}\sin^2\theta_t + \frac{2}{3}s_w^2 \cos 2\theta_t\right) + m_t^2 + \frac{1}{2}m_t X_t \sin 2\theta_t, \tag{11}$$

where θ_t is the mixing angle between the flavor basis and mass eigenbasis,

$$\sin 2\theta_t = -\frac{2m_t X_t}{m_{\tilde{t}_1}^2 - m_{\tilde{t}_2}^2}, \quad \cos 2\theta_t = \frac{m_{\tilde{t}_L}^2 + D_L^t - m_{\tilde{t}_R}^2 - D_L^t}{m_{\tilde{t}_1}^2 - m_{\tilde{t}_2}^2}, \tag{12}$$

such that

$$\begin{pmatrix} \cos\theta_t & -\sin\theta_t \\ \sin\theta_t & \cos\theta_t \end{pmatrix} M_{\tilde{t}}^2 \begin{pmatrix} \cos\theta_t & \sin\theta_t \\ -\sin\theta_t & \cos\theta_t \end{pmatrix} = \begin{pmatrix} m_{\tilde{t}_1}^2 & 0 \\ 0 & m_{\tilde{t}_2}^2 \end{pmatrix}. \tag{13}$$

The form factors $A_0^h(\tau)$ and $A_{\frac{1}{2}}^h(\tau)$ approach 4/3 and 1/3, respectively, for $\tau_i = m_h^2/(4m_i^2) \to 0$. For $m_h \sim 120$ GeV, $m_t = 172$ GeV, and $m_{\tilde{t}} \sim 200$ GeV, one can check that $\tau \to 0$ is a good approximation for the form factors.

The $\tau_i \to 0$ limit is equivalent to approximating the one-loop diagram in Fig. 1 by a dimension-five local operator $(h/v)G^a_{\mu\nu}G^{a\,\mu\nu}$, whose coefficient has long been known to be related to the QCD one-loop beta function [13, 14]. If we turn on a background Higgs field h and consider the squark threshold effect for the running of one-loop beta function of QCD, neglecting other contributions for now, we get

$$\begin{aligned} -\frac{1}{4g^2(\mu_{\rm r})}G^a_{\mu\nu}G^{a\,\mu\nu} &= -\frac{1}{4}\left(\frac{1}{g^2(\Lambda)} - \frac{b_3^{\rm UV}}{16\pi^2}\log\frac{\Lambda^2}{\mu_{\rm r}^2} - \sum_{i=1,2}\frac{b_3^{(0)}}{16\pi^2}\log\frac{m_{\tilde{t}_i}^2(h)}{\mu_{\rm r}^2} - \cdots\right) G^a_{\mu\nu}G^{a\,\mu\nu} \\ &= -\frac{1}{4}\left(-\frac{b_3^{(0)}}{16\pi^2}\log\frac{\det M_{\tilde{t}}^2(h)}{\mu_{\rm r}^2} - \cdots\right) G^a_{\mu\nu}G^{a\,\mu\nu}, \end{aligned} \tag{14}$$

where $b_3^{(0)} = 1/6$ [15]. Expanding $\det M_{\tilde{t}}^2(h)$ in the presence of the background Higgs field h with respect to $\langle h\rangle = v/\sqrt{2}$, one immediately obtains the dimension-five operator $(h/v)G^a_{\mu\nu}G^{a\,\mu\nu}$, whose coefficient is essentially determined by the quantity

$$v\frac{\partial}{\partial h}\log\det M_{\tilde{t}}^2(h)\Big|_{h=v/\sqrt{2}}. \tag{15}$$

In fact, it is straightforward to verify in Eq. (6) that in the limit $\tau_i \to 0$ the stop contribution to the decay width $\Gamma(h \to gg)$ is controlled by

$$\begin{aligned} \sum_{i=1,2}\frac{g_{h\tilde{t}_i\tilde{t}_i}}{m_{\tilde{t}_i}^2} &= \frac{m_{\tilde{t}_1}^2 g_{h\tilde{t}_2\tilde{t}_2} + m_{\tilde{t}_2}^2 g_{h\tilde{t}_1\tilde{t}_1}}{\det M_{\tilde{t}}^2}, \\ &= \frac{1}{2}\, v\frac{\partial}{\partial h}\log\det M_{\tilde{t}}^2(h)\Big|_{h=v/\sqrt{2}}. \end{aligned} \tag{16}$$

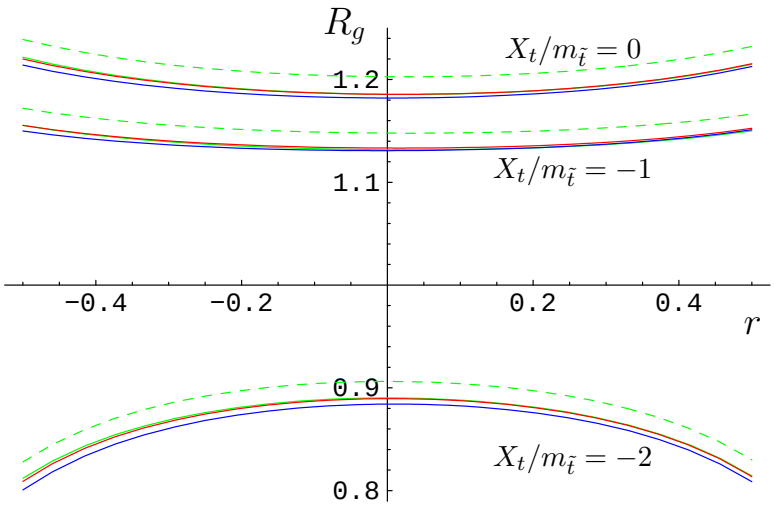

FIG. 2: Plot of R_g as a function of r for $m_{\tilde{t}}^2 = 500$ GeV, $\tan\beta = 10$ (green/gray), $\tan\beta = 30$ (red/dark gray), $\tan\beta = 50$ (blue/black). The solid lines are for other SUSY masses fixed to 400 GeV. For comparison, the (green/gray) dashed lines are for other SUSY masses fixed to 800 GeV and $\tan\beta = 10$. The three clusters of lines correspond to $X_t/m_{\tilde{t}} = 0, -1, -2$ as indicated in the plot.

If we further drop the subleading contribution proportional to m_Z^2 in $g_{h\tilde{t}_i\tilde{t}_i}$, then Eq. (16) becomes

$$\frac{m_t^2(m_{\tilde{t}_1}^2 + m_{\tilde{t}_2}^2) + m_t^2 X_t^2}{\det M_{\tilde{t}}^2}. \tag{17}$$

Defining the variables

$$m_{\tilde{t}}^2 = \frac{m_{\tilde{t}_L}^2 + m_{\tilde{t}_R}^2}{2}, \quad r = \frac{m_{\tilde{t}_L}^2 - m_{\tilde{t}_R}^2}{m_{\tilde{t}_L}^2 + m_{\tilde{t}_R}^2}, \tag{18}$$

then Eq. (17) depends mostly on X_t and $m_{\tilde{t}}^2$, and weakly on r which only appears in the denominator. In Fig. 2 we demonstrate that R_g, the ratio of the full gluon fusion rate in the MSSM over the rate in the standard model, varies little for $|r| \lesssim 0.4$. The value of $r = 0.4$ for $m_{\tilde{t}} = 500$ GeV corresponds to $m_{\tilde{t}_L} \sim 590$ GeV and $m_{\tilde{t}_R} \sim 390$ GeV. Most SUSY breaking scenarios generate comparable $m_{\tilde{t}_L}$ and $m_{\tilde{t}_R}$, and since the renormalization group running of stop masses is dominated by the gluino mass, the contribution of which is identical for both $m_{\tilde{t}_L}$ and $m_{\tilde{t}_R}$, the weak scale values of both masses remain close to each other. For example, all the SPS benchmark scenarios for supersymmetry in Ref. [16] have stop mass splittings that fall within $|r| \leq 0.4$. Throughout this paper we use the publicly available code `FeynHiggs2.5` [17] in numerical computation and making the plots.

In Fig. 2 we plot the production rate for $\tan\beta = 10$, 30, 50 (although these three cases are plotted with different color/shades they are hard to distinguish because of the negligible dependence on $\tan\beta$) and two different common masses of all other superpartners, 400 GeV (solid) and 800 GeV (dashed, only for $\tan\beta = 10$). The three clusters of lines correspond to $X_t/m_{\tilde{t}} = 0, -1, -2$ as indicated in the plot. It is clear that the dependence on $\tan\beta$ and masses of other superpartners is very small.

IV. STOPS AND THE HIGGS MASS

In the Higgs sector of MSSM there are two Higgs doublets, H_u and H_d, coupling to the up-type and down-type quarks respectively. After electroweak symmetry breaking three components are eaten Goldstone bosons and give mass to the electroweak gauge bosons through the Higgs mechanism. The remaining physical states are two CP-even neutral Higgs bosons, h (the lighter one) and H (the heavier one), one CP-odd neutral Higgs boson A, and the charged Higgses $H^{\pm}$. In MSSM supersymmetry imposes very tight constraints on the Higgs potential at tree-level, in particular, the scalar quartic couplings are completely fixed by $SU(2)_w \times U(1)_Y$ gauge couplings. As a result there are two free parameters in the MSSM Higgs sector, usually taken to be $\tan\beta$ and m_A, and one can derive hierarchical relations for masses of different Higgs bosons [8]. Among them the most important one is perhaps the upper bound on the mass of the lightest Higgs boson h,

$$m_h \leq m_Z |\cos 2\beta| \leq m_Z = 91.2 \ \ \text{GeV}, \tag{19}$$

which is clearly below the LEP bound $m_h \geq 114$ GeV.

Therefore, one usually resorts to large radiative corrections from superpartners with significant coupling to the Higgs boson to raise m_h. This is why m_h is most sensitive to the parameters in the stop sector, and not to masses of other superparticles. [4] For simplicity if we assume $m_{\tilde{t}_R} \simeq m_{\tilde{t}_L} = m_{\tilde{t}}$, the one-loop correction to m_h is approximately given as

$$\Delta m_h^2 \simeq \frac{3G_F}{\sqrt{2}\pi^2} m_t^4 \left\{ \log\frac{m_{\tilde{t}}^2}{m_t^2} + \frac{X_t^2}{m_{\tilde{t}}^2}\left(1 - \frac{X_t^2}{12 m_{\tilde{t}}^2}\right)\right\}, \tag{20}$$

which grows logarithmically with the stop mass $m_{\tilde{t}}$. On the other hand, because of the

[4] The exception is again the sbottom sector for very large $\tan\beta$ and large μ.

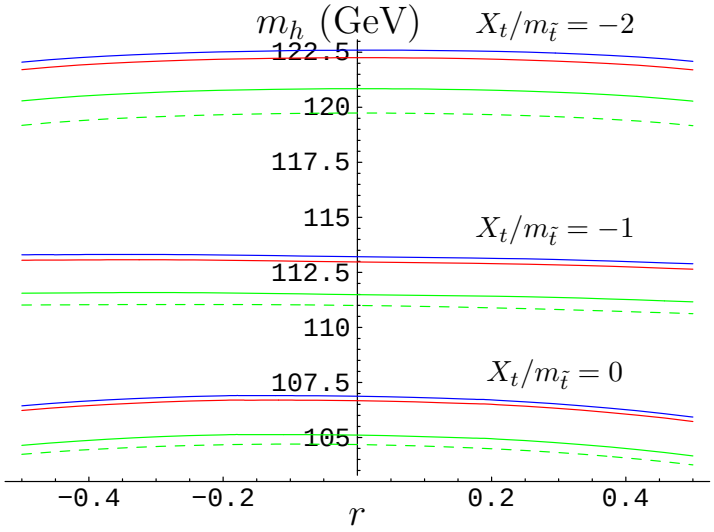

FIG. 3: Plot of the Higgs boson mass as a function of r for $m_{\tilde{t}}^2 = 500$ GeV, $\tan\beta = 10$ (green/gray), $\tan\beta = 30$ (red/dark gray), $\tan\beta = 50$ (blue/black). The solid lines are for other SUSY masses fixed to 400 GeV. For comparison, the (green/gray) dashed lines are for other SUSY masses fixed to 800 GeV and $\tan\beta = 10$. The three clusters of lines correspond to $X_t/m_{\tilde{t}} = 0, -1, -2$ as indicated in the plot.

quadratic divergence the up-type Higgs mass increases with $m_{\tilde{t}}^2$,

$$\Delta m_{H_u}^2 \simeq -\frac{3}{8\pi^2} m_{\tilde{t}}^2 \log\frac{\Lambda^2}{m_{\tilde{t}}^2}. \tag{21}$$

It is the logarithmic versus quadratic dependence on the stop mass that dictates the fine-tuning in MSSM. For $m_{\tilde{t}_R} \simeq m_{\tilde{t}_L}$ the stop masses need to be very large, $\mathcal{O}(1\text{ TeV})$, to evade the LEP limit on the Higgs mass, which leads to large ($\mathcal{O}(m_Z^2/m_{\tilde{t}}^2) \lesssim 1\%$) fine-tuning in electroweak symmetry breaking. On the other hand, the stop masses could be significantly below 1 TeV if there is large mixing in the stop sector, in which case the fine tuning can be reduced to the level of 5%. The Higgs mass is maximized for $|X_t/m_{\tilde{t}}| \sim 2$ and with this mixing light stops, $m_{\tilde{t}_R} \simeq m_{\tilde{t}_L} \simeq 300$ GeV, are sufficient to push the Higgs mass above the LEP limit.

From the discussion above, we see that for $\tan\beta \gtrsim 10$ the tree level contribution to the Higgs mass is saturated and the residual dependence of the Higgs mass on $\tan\beta$ is very weak ($\tan\beta$ does not enter the leading one loop correction). Furthermore, in spite of Eq. (20) being derived for $m_{\tilde{t}_R} \simeq m_{\tilde{t}_L}$ and the Higgs mass in general being dependent on all three parameters in the stop sector: $m_{\tilde{t}}$, X_t and r, the dependence on r is very weak for quite

large deviations of $m_{\tilde{t}_R}$ and $m_{\tilde{t}_L}$ from the average value. In Fig. 3 we plot the sensitivity of the Higgs mass to r for three different values of $\tan\beta$ (distinguished by colors/shades) and two different common masses of all other superpartners, 400 GeV (solid) and 800 GeV (dashed, only for $\tan\beta = 10$). The three clusters of lines correspond to $X_t/m_{\tilde{t}} = 0, -1, -2$ as indicated in the plot. Again we see that m_h is not much dependent of r, $\tan\beta$, and masses of other superpartners in the region of parameter space we are considering.

V. RESULTS

In this section we present our results, concentrating on the observables m_h and $R_g \equiv \Gamma_g^{\rm MSSM}/\Gamma_g^{\rm SM}$ which is the ratio of the Higgs production rate in the gluon fusion channel in the MSSM and in the standard model. Contours of constant m_h and R_g are plotted in the $m_{\tilde{t}} - X_t/m_{\tilde{t}}$ plane, as shown in Fig. 4.

Let us focus first on the contours of constant R_g, observing that $R_g \gtrsim 1$ when the mixing in the stop sector is small $|X_t/m_{\tilde{t}}| \lesssim 1.6$ regardless of $m_{\tilde{t}}$. Moreover, for small mixing R_g increases as $m_{\tilde{t}}$ decreases, since lighter stops give more significant contributions to the production rate. On the other hand, in the region where stops are light $m_{\tilde{t}} \sim \mathcal{O}(500\ \text{GeV})$ and mixing is large $|X_t/m_{\tilde{t}}| \sim 2$, we see $R_g \lesssim 1$. The fact that the Higgs production in the gluon fusion channel in the MSSM could be smaller than in the standard model for large mixing in the stop sector has previously been observed in Ref. [10]. It is interesting to note that R_g alone seems to give a good sense of the magnitude of $X_t/m_{\tilde{t}}$: $R_g \gtrsim 1$ if the mixing is small and $R_g \lesssim 1$ if the mixing is large.

For contours of constant Higgs mass, the story is similar to what has been said repeatedly in the literature. If there is no mixing in the stop sector, the stop mass $m_{\tilde{t}}$ needs to be close to 1 TeV in order to have a Higgs mass above the LEP bound of 114 GeV. The Higgs mass starts increasing when one turns on the mixing and eventually reaches a maximum value for $|X_t/m_{\tilde{t}}| \sim 2$. In the region of large mixing light stops, $m_{\tilde{t}} \simeq 300$ GeV, are still allowed by $m_h \geq 114$ GeV.

When we consider both kinds of contours altogether, there are several observations to be made. First consider the region of small mixing. In this region contours of constant m_h and R_g run somewhat parallel to each other vertically, implying a very loose constraint on $m_{\tilde{t}}$, the overall stop mass scale, unless the gluon production rate can be measured precisely in

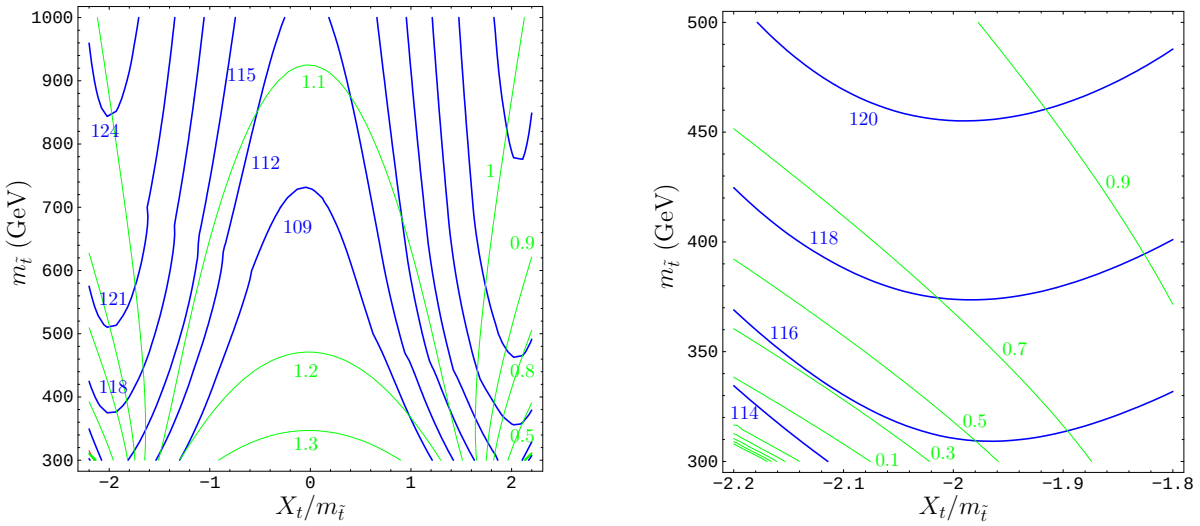

FIG. 4: Contours of constant Higgs mass m_h (GeV) (blue/black) and the gluon fusion rate R_g (green/gray) in $m_{\tilde{t}}$ – $X_t/m_{\tilde{t}}$ plane. The plot on the right zooms in on the region of small $m_{\tilde{t}}$ and large mixing $X_t/m_{\tilde{t}}$. All other SUSY masses are fixed to 400 GeV, $\tan\beta = 10$ and $\mu = 200$ GeV.

experiments. Furthermore, the region where $R_g \gtrsim 1$ corresponds to the region where EWSB is more fine-tuned. Once we move into the region where $R_g \lesssim 1$, contours of constant R_g run at large angles with contours of constant m_h, which means it is possible to determine both $m_{\tilde{t}}$ and $X_t/m_{\tilde{t}}$ fairly well even if there is a large uncertainty in R_g. This is because in this region R_g is quite sensitive to $m_{\tilde{t}}$ and (especially) $X_t/m_{\tilde{t}}$, and decreases rapidly with increasing mixing and decreasing stop masses. Therefore measurements of m_h and R_g will allow for a fairly accurate determination of $m_{\tilde{t}}$ and $X_t/m_{\tilde{t}}$ in the region of large mixing and light stops. All these measurements involve properties of the Higgs boson and can be done without prior knowledge of other masses and mixing angles in the MSSM spectrum. As demonstrated in previous sections, these results are not sensitive to other parameters, and choosing different values of $\tan\beta$, μ or masses of other superpartners would only negligibly change results presented in Fig. 4.

In Fig. 4 we have also zoomed in on the region of large mixing with negative X_t and small stop mass, since this is the region of particular interest: both m_h and R_g vary rapidly. This is also the least fine-tuned region of MSSM. From the zoomed in plot one can see that, for example, if the experimental central values are $m_h = 118$ GeV and $R_g = 0.7$, then the corresponding central values for $m_{\tilde{t}}$ and $X_t/m_{\tilde{t}}$ will be 380 GeV and -2, respectively. Of course we should not forget that there is another solution for roughly the same $m_{\tilde{t}}$ but

positive $X_t/m_{\tilde{t}}$. We also mention in passing that all the constant R_g contours re-appear in the dense region near the bottom-left corner [5] where $m_{\tilde{t}} \sim 300$ GeV and $X_t/m_{\tilde{t}} \sim -2.2$. They re-appear because in this region the lightest stop is extremely light in the order of 120 GeV, for which the stop contribution in the gluon fusion rate, Eq. (6), completely overwhelms the standard model contribution. Therefore the production rate at first decreases all the way to zero, when stop contribution reaches a critical value and become equal and opposite to the top contribution, and then starts growing when stop contribution becomes more negative than the critical value. In this region R_g is a very rapidly growing function for decreasing stop mass. The end result is a region with very densely populated contours in the very bottom-left corner in Fig. 4.

At this point we would like to comment on various theoretical and experimental uncertainties one might encounter in implementing our strategy. For the lightest CP-even Higgs boson h, if it is observed in the golden channel $h \to ZZ \to \ell^+\ell^-\ell^+\ell^-$ or the silver mode $h \to \gamma\gamma$, then its mass can be measured with an accuracy of $\Delta m_h/m_h \sim 0.2\%$ at the LHC [18]. For $m_h \sim 120$ GeV, this gives an uncertainty of only 250 MeV! Unfortunately, the theoretical uncertainty in computing m_h within MSSM is still quite large in comparison. In the MSSM the full one-loop and dominant two-loop corrections to m_h have been calculated, however, results from two different renormalization schemes differ by about $2-3$ GeV [8]. The difference can be seen as a rough estimate of the magnitude of the unknown higher order corrections. On the other hand, the situation with uncertainties in the partial width $\Gamma(gg \to h)$, and hence R_g, is less optimistic. The reason is two-fold. First the production rate of $gg \to h$ is not directly measurable in experiments since the Higgs can only be seen through its decay products. Instead, what can be measured directly is the cross-section times the branching ratio such as $\sigma(gg \to h) \times \mathrm{Br}(h \to 2\gamma)$. By combining measurements on Higgs production and decay in different channels it is possible to extract individual partial decay width, and at the LHC with a 200 fb^{-1} luminosity the error is expected to be $\Delta\Gamma_g/\Gamma_g \sim 30\%$ when including systematic errors of approximately 20% from higher order QCD corrections [19, 20].

In the end, the uncertainty in m_h is expected to be at the level of 2%, dominated completely by theoretical uncertainty, whereas the uncertainty in R_g is much larger, at the level

[5] In fact, in this region $m_h < 114$ GeV which is ruled out by the LEP limit.

of 30%. However, we should stress that, even with a 30% uncertainty in R_g, in the region of large mixing and small stop mass it could still be useful to apply our strategy due to the fact that R_g is very sensitive to $m_{\tilde{t}}$ and X_t in this region. For example, even if the production rate is poorly measured to be in the region $0.7 \gtrsim R_g \gtrsim 0.3$, it is still possible to constrain the $m_{\tilde{t}} - X_t/m_{\tilde{t}}$ plane down to a small area by knowing m_h with 2 GeV uncertainty, as can be seen from Fig. 4.

VI. THE SANITY OF THE MSSM

Next we use the results in the previous section to explore the interesting possibility that measurements of the Higgs mass and the production rate do not have overlapping contours in the $m_{\tilde{t}} - X_t/m_{\tilde{t}}$ plane. Both m_h and R_g is a measure on the overall stop mass scale $m_{\tilde{t}}$ and the mixing X_t. If somehow the $m_{\tilde{t}}$ and X_t inferred separately from m_h and R_g are very far off, then it is a signal that the region of parameter space we are considering,

$$10 \lesssim \tan\beta \lesssim m_t/m_b, \quad m_b\,|\mu \tan\beta| \;\lesssim\; m^2_{\tilde{b}_L},\; m^2_{\tilde{b}_R}, \quad \text{and} \quad |r| \lesssim 0.4, \tag{22}$$

is disfavored. In this case, we can further ask if it is possible to reconcile the differences in these two measurements by considering other parameter regions.

From Fig. 4 we see that the only situation in which contours from measurements of the Higgs mass and the production rate would not overlap (taking into account uncertainties discussed in the previous section) is when the Higgs is relatively heavy, $m_h \gtrsim 130$ GeV, and production rate very small, $R_g \lesssim 0.6$. This is a conflict in that a heavy Higgs mass around 130 GeV requires a high stop mass scale, $m_{\tilde{t}} \gtrsim 1$ TeV, whereas a small production rate prefers a low stop mass scale, $m_{\tilde{t}} \lesssim 500$ GeV.

In order to find a resolution in these two measurements, it is necessary to find ways to lower $m_{\tilde{t}}$ while keeping m_h fixed at around 130 GeV, or increase $m_{\tilde{t}}$ while maintaining a small R_g at roughly 0.6. Immediately we conclude that going to a smaller $\tan\beta$ would not help because, in this case, the tree-level contribution to the Higgs mass is reduced and $m_{\tilde{t}}$ has to be even higher in order to produce a larger radiative corrections to keep m_h large. This worsens the discrepancy.

An alternative is to have a large $\tan\beta \sim m_t/m_b$ for which the sbottoms contributions are important and it is helpful to first discuss the effect of sbottoms on both the Higgs mass

and the production rate. In the decoupling limit, a large $\tan\beta$ is only a necessary but not a sufficient condition for the sbottoms effects to be important in the Higgs mass; a sizable μ term is also required. In this case the mixing in the sbottom sector can be very large which has a tendency to decrease the Higgs mass [9]. Obviously larger μ term causes even larger X_b and therefore smaller Higgs mass. Moreover the Higgs mass is not an even function in $X_b \to -X_b$ and hence not in $\mu \to -\mu$ either.[6] For the Higgs production in the gluon fusion channel, since the sbottoms mass matrix and its couplings to the lightest CP-even Higgs is very similar to those of the stops in Sect. III with the corresponding electroweak charges, masses, and mixing term replaced by those from the sbottoms, we expect that, in the same fashion as the stops, if the sbottoms are light and mixing large, they could decrease the production of the Higgs in the gluon fusion channel. The production rate does not depend explicitly on the sign of X_b but only implicitly through the Higgs mass m_h.

Now in order to produce a large effect in the production rate the sbottom has to be light, since its contribution decouple as $1/m_{\tilde{b}}^2$. On the other hand, the stop must be heavy to keep the Higgs mass large. At this point it is important to keep in mind that the soft-breaking masses for the left-handed sfermions are required to be the same by the $SU(2)_w$ gauge symmetry: $m_{\tilde{t}_L}^2 = m_{\tilde{b}_L}^2 = m_{\tilde{q}_3}^2$. Therefore there is a limited number of ways to keep at least one of the sbottoms light and at least one of the stops heavy. As an example, $m_h \sim 130$ GeV and $R_g \sim 0.6$ can be produced with the following choices of parameters (assuming large mixing in the stop sector that maximizes m_h):

(a) $\tan\beta \sim 50$, $m_{\tilde{q}_3} \sim m_{\tilde{t}_R} \sim 2000$ GeV, $m_{\tilde{b}_R} \sim 100$ GeV, and $\mu \sim -800$ GeV,[7]

(b) $\tan\beta \sim 50$, $m_{\tilde{q}_3} \sim m_{\tilde{b}_R} \sim 300$ GeV, $m_{\tilde{t}_R} \sim 5000$ GeV, and $\mu \sim -250$ GeV,

and small variations of these. As one can see, reconciling these two measurement in m_h and R_g, by going outside of the choices of parameters we considered in Eq. (22), would require huge hierarchies in and between the stop and sbottom sectors. Such hierarchies are difficult to generate from a sensible UV model and we consider them extreme and rather insane. The more plausible explanation of conflicting values of m_h and R_g would be contributions from physics beyond the MSSM.

[6] Notice that our definition of μ differs from that in [9] by a sign.

[7] In this case the lightest sbottom $\tilde{b}_1$ is slightly lighter than 100 GeV. However, if $\tilde{b}_1$ is mostly right-handed, which is the case here, the limit on its mass is very weak, much lower than 100 GeV [21].

VII. DISCUSSION AND CONCLUSIONS

In this paper we proposed using the Higgs boson as a probe of the stop sector. Our method relies on measurements of the Higgs mass as well as the production rate in the gluon fusion channel, the dominant production channel at the LHC. For $m_t/m_b \gtrsim \tan\beta \gtrsim 10$ and small μ term, our proposal is insensitive to other mass parameters in the MSSM and thus complementary to the conventional method of studying the production and decay processes of stops, which requires knowledge of masses and mixing angles in the chargino and neutralino sector.

In the stop mass-squared matrix, there are three free parameters $m^2_{\tilde{t}_L}, m^2_{\tilde{t}_R}$ and X_t which (roughly) correspond to the two diagonal entries and the one off-diagonal entry. With only two measurements, the Higgs mass and the production rate in the gluon fusion channel, one might expect that a priori it is only possible to constrain the three parameters on a one-dimensional surface. Nevertheless, we demonstrated that both measurements are sensitive to only two out of the three parameters in the mass matrix; there is a (almost) flat direction in the space of parameters. In the end two measurements provide access to, in terms of variables defined in Eq. (18), the overall stop mass scale $m^2_{\tilde{t}}$ and the mixing term X_t, as long as $|r| \leq 0.4$. It is worth pointing out that all the Snowmass benchmark scenarios for MSSM have mass splittings satisfying $|r| \leq 0.4$. We also note that very often r is calculable from a given UV model in which case it is not a free parameter and our procedure can be used to determine the stop sector of the model completely.

The proposed strategy is the least effective when the mixing in the stop sector is not large, for in this region contours of two different measurements run in parallel to each other. This happens when the Higgs is light and the production rate is close to the standard model value. On the other hand, our method is the most effective when stops are light and the mixing is large, in which case the allowed area in the $m_{\tilde{t}} - X_t/m_{\tilde{t}}$ plane is quite small. Because the production rate is very sensitive to $m_{\tilde{t}}$ and X_t in this particular region, even with an uncertainty as large as 30% in the production rate, our proposal could be useful as discussed in the previous section.

We also considered the case when there is a discrepancy between the measurements of the Higgs mass and the production rate. This could happen if the lightest CP-even Higgs is heavy, $m_h \gtrsim 130$ GeV, and the production rate is significantly smaller than in the standard

model. Even though it is possible to generate such a pattern in the MSSM, the required spectrum has large mass hierarchies in and between the stop and sbottom sectors which resides in extreme corners of the parameter space.

As a final comment, the effectiveness of our strategy is clearly limited by the possibly large uncertainty incurred in the measurement of the production rate in the gluon fusion channel. We hope our proposal could serve as a strong motivation to make an effort to reduce the uncertainty in the gluon fusion production rate, either through a better experimental measurement or a more precise theoretical calculation. Before that goal is achieved, a better observable to consider is probably the event rate of $gg \to h \to \gamma\gamma$, which is directly measurable and has less uncertainty. However, the decay rate to two photons in the MSSM depends not just on stop masses but also on chargino masses. Thus if charginos are observed at the LHC and their masses are measured, then it could be useful to combine the measurement of $gg \to h \to \gamma\gamma$ with the Higgs mass, in the same fashion as described in this paper, to constrain the stop sector of the MSSM.

Acknowledgments

We thank Thomas Hahn and Sven Heinemeyer for help and correspondences on `FeynHiggs`. RD thanks Hyung Do Kim for useful discussions. This work is supported in part by the Department of Energy under grant DE-FG02-90ER40542.

---

[1] See, for example, LEP Higgs Working Group, LHWG-NOTE-2005-01.

[2] R. Dermisek and J. F. Gunion, Phys. Rev. Lett. **95**, 041801 (2005) [arXiv:hep-ph/0502105].

[3] K. Choi, K. S. Jeong, T. Kobayashi and K. i. Okumura, Phys. Lett. B **633**, 355 (2006) [arXiv:hep-ph/0508029].

[4] R. Kitano and Y. Nomura, Phys. Lett. B **631**, 58 (2005) [arXiv:hep-ph/0509039].

[5] R. Dermisek and H. D. Kim, Phys. Rev. Lett. **96**, 211803 (2006) [arXiv:hep-ph/0601036].

[6] R. Dermisek, H. D. Kim and I. W. Kim, JHEP **0610**, 001 (2006) [arXiv:hep-ph/0607169].

[7] See, for example, G. Weiglein *et al.* [LHC/LC Study Group], Phys. Rept. **426**, 47 (2006) [arXiv:hep-ph/0410364].

[8] For a recent review see A. Djouadi, arXiv:hep-ph/0503173.

[9] A. Brignole, G. Degrassi, P. Slavich and F. Zwirner, Nucl. Phys. B **643**, 79 (2002) [arXiv:hep-ph/0206101].

[10] A. Djouadi, Phys. Lett. B **435**, 101 (1998) [arXiv:hep-ph/9806315].

[11] H. E. Haber, arXiv:hep-ph/9505240.

[12] For a recent review see A. Djouadi, arXiv:hep-ph/0503172.

[13] J. R. Ellis, M. K. Gaillard and D. V. Nanopoulos, Nucl. Phys. B **106**, 292 (1976).

[14] M. A. Shifman, A. I. Vainshtein, M. B. Voloshin and V. I. Zakharov, Sov. J. Nucl. Phys. **30**, 711 (1979) [Yad. Fiz. **30**, 1368 (1979)].

[15] D. R. T. Jones, Phys. Rev. D **25**, 581 (1982).

[16] B. C. Allanach *et al.*, arXiv:hep-ph/0202233.

[17] S. Heinemeyer, W. Hollik and G. Weiglein, Comput. Phys. Commun. **124**, 76 (2000) [arXiv:hep-ph/9812320].

[18] M. Della Negra et. al., "CMS physics : Technical Design Report v.2 : Physics performance," CERN-LHCC-2006-021.

[19] D. Zeppenfeld, arXiv:hep-ph/0203123.

[20] A. Belyaev and L. Reina, JHEP **0208**, 041 (2002) [arXiv:hep-ph/0205270].

[21] M. Carena, S. Heinemeyer, C. E. M. Wagner and G. Weiglein, Phys. Rev. Lett. **86**, 4463 (2001) [arXiv:hep-ph/0008023].